Analysis of Schottky contact formation in coplanar Au/ZnO/Al nano-gap RF diodes processed from solution at low temperature

*James Semple, Stephan Rossbauer, Thomas D. Anthopoulos**

Department of Physics and Centre for Plastic Electronics
Blackett Laboratory, Imperial College London, London SW7 2AZ, United Kingdom
Corresponding author e-mail: t.anthopoulos@ic.ac.uk

KEYWORDS
Planar Schottky diode; adhesion lithography; Richardson constant; solution processing; ZnO; radio frequency diode; RFID

ABSTRACT

Much work has been carried out in recent years in fabricating and studying the Schottky contact formed between various metals and the *n*-type wide bandgap semiconductor zinc oxide (ZnO). In spite of significant progress, reliable formation of such technologically interesting contacts remains a challenge. Here, we report on solution-processed ZnO Schottky diodes based on a coplanar Al/ZnO/Au nano-gap architecture and study the nature of the rectifying contact formed at the ZnO/Au interface. Resultant diodes exhibit excellent operating characteristics, including low-operating voltages (±2.5 V) and exceptionally high current rectification ratios of $>10^6$ that can be independently tuned via scaling of the nano-gap's width. The barrier height for electron injection responsible for the rectifying behaviour is studied using current-voltage-temperature and capacitance-voltage measurements (C-V) yielding values in the range of 0.54-0.89 eV. C-V measurements also show that electron traps present at the Au/ZnO interface appear to become less significant at higher frequencies, hence making the diodes particularly attractive for high frequency applications. Finally, an alternative method for calculating the Richardson constant is presented yielding a value of 38.9 A cm^{-2} K^{-2} which is close to the theoretically predicted value of 32 A cm^{-2} K^{-2}. The implications of the obtained results for the use of these coplanar Schottky diodes in radio frequency applications is discussed.

1. Introduction

For over a decade, zinc oxide (ZnO) has been at the center of significant research efforts, owing to its optical transparency and its potential utilization in a range of opto/electronics including Schottky diodes[1–3] , lasers[4] , thin-film transistors (TFTs)[5] and piezoelectric devices.[6] Schottky diodes, in particular, are currently receiving increasing attention due to their potential for application in radio frequency (RF) electronics, optoelectronics and high power electronics but also because they present an interesting platform for material characterization.[7–9] Because of these attributes recent research has been devoted to the development of high quality ZnO-based Schottky diodes manufactured using a range of processing techniques and contact materials.

In an ideal metal-semiconductor (M-S) junction, the barrier height for electron injection (Φ_B) depends primarily on the metal work function (Φ_M) and the electron affinity of the semiconductor (χ_S), and is given by the Schottky-Mott equation:

$$\Phi_B = \Phi_M - \chi_S \tag{1}$$

However, practical devices have long been known to deviate from this ideal behaviour, owing to imperfect materials interactions at M-S interface including Fermi level pinning at the semiconductor surface due to dangling bonds and image force lowering.[10,11] The case of ZnO is no exception. With an electron affinity of ~4.2 eV, Schottky barriers with noble metals such as Au (4.8-5.2 eV), would be expected to yield potential barrier height of up to 1 eV. However, typical values reported in the literature fall in the range of 0.6-0.8 eV.[12–14] Understanding the underlying reasons for this non-ideal device behaviour is therefore critical for exploiting this rather promising device technology for real life opto/electronic applications.

It is known that the depletion region width (w) in Schottky diodes is on the order of nanometers and depends on the semiconductor material employed.[15] Thus diodes based on semiconducting layers with thickness (d) > w exhibit larger RC constants due to additional series resistance. Although reduction in the semiconductor layer thickness may in principle allow realization of Schottky diodes with improved operating characteristics, fabricating such thin semiconductor layer-based diodes is difficult, particularly when solution-processable semiconductors are employed. This is because the two metal electrodes tend to short through defects in the thin semiconductor layer and/or through unintentional doping of the semiconductor caused by metal migration occurring during top contact deposition. Use of coplanar diode architectures in which the Ohmic and the Schottky contact electrodes are patterned next to each other at an inter-electrode distance of <w, could provide a solution to this manufacturing bottleneck. However producing such nano-gap devices is not trivial owing to the complexity of fabricating asymmetric electrodes with inter-electrode distances on the order of w.

Recently, we reported the development of coplanar Schottky diodes based on ZnO layers processed from solution at low temperatures (<200 °C).[16] These coplanar diodes feature asymmetric Al/Au metal electrodes separated by ≤ 20 nm (nano-gap)[17] and a thin layer of ZnO (<20 nm) which is solution-deposited on top.[16] Due to the extreme dimensionality and the coplanar nature of the device architecture, the ZnO diodes are able to operate at high frequencies enabling their integration in RF rectifying circuits manufactured on arbitrary substrates including plastic.[16] Despite their excellent potential, however, little is known about the all-important Au/ZnO interface that gives rise to the highly current rectifying behavior observed. Therefore, understanding the mechanism of electron injection at the Au/ZnO interface, would provide

valuable knowledge that could be used to further advance this interesting device concept as well as help to identify associated technology bottlenecks, if any.

Here we investigate the electrical properties of solution-deposited ZnO Schottky nano-gap diodes comprised of coplanar asymmetric Au/Al electrodes using different electrical characterization techniques. We show that the coplanar device architecture helps to negate the unwanted effects of metal diffusion and electrical shorting through the semiconductor layer, while maintaining the junction capacitance at ultra-low levels (~pF). As-prepared Schottky diodes exhibit low-voltage operation (<2.5 V) and unprecedented current rectification ratio (>10^6) which can be increased further through appropriate device size scaling. The barrier height for electron injection at Au/ZnO interface is extracted using direct current (DC) and alternating current (AC) characterisation techniques yielding values in the range of 0.54-0.89 eV. Interestingly, diode performance is found to improve at higher operating frequencies, an effect attributed to the reduction of electron trapping within ZnO. The implications of this interesting characteristic are discussed in light of possible technological applications in radio frequency (RF) electronics.

2. Methods

Aluminium/gold (Al/Au) nano-gap electrodes were patterned employing our recently reported adhesion lithography (a-Lith) technique.[17] The resultant structures were circular gold electrodes with a circumference of roughly 1 mm separated from a host phosphonic acid self-assembled monolayer (SAM) coated Al electrode by <20 nm. The SAM was subsequently removed by subjecting the samples to 10 minutes UV-ozone treatment. **Figure 1(A)** shows the schematic of

the coplanar nanojunction Schottky diode array and the cross-section of a single device, while in **Figure 1(B)** we show the energy band diagram of the Schottky contact expected to form between Au and ZnO. Following the patterning of the asymmetric Al/Au nano-gap electrodes, a precursor solution of zinc oxide hydrate dissolved in ammonium hydroxide (0.25 M concentration) was spin coated directly onto the Au/Al electrodes array in ambient conditions, followed by thermal annealing of the sample at 200 °C in air for 30 min. Further details on the materials preparation and deposition can be found elsewhere.[5,18] Electrical characterization of the diodes was performed in a nitrogen atmosphere using a Keithley 4200 semiconductor parameter analyzer, while temperature dependent current-voltage (I-V-T) and capacitance-voltage (C-V) measurements were carried out in high vacuum of 10^{-5} mbar using a Janis cryogenic probe station. The ultra-thin nature of the overlaying solution processed ZnO semiconducting layer (<10 nm) [16] allows for easy contact of the asymmetric Au/Al electrodes with tungsten microprobes probes (10 μm apex diameter).

3. Results & Discussion

3.1. Room-Temperature Current-Voltage Characteristics

In **Figure 1 (C)** we show the semi-logarithmic plot of an I-V characteristic measured for a representative coplanar ZnO diode with channel width/circumference (w) and inter-electrode distance (nano-gap) of 1 mm and ~20 nm, respectively. Inset displays a microscope image of the actual Schottky diode array characterized. The device exhibits low-voltage operation (±2.5 V) and excellent current rectification of $>10^6$ with a forward bias current exceeding 0.1 mA at +2.5 V, despite its small 'active' area. To the best of our knowledge, this is the highest rectification

ratio value reported to date for a solution-processed metal oxide diode. To this end, the rectification ratio of solution processed ZnO diodes typical fall in the range of 10-10^3.[1,19–28] For example, Chen *et al*. [29] reported rectification ratios in excess of 10^4 for diodes processed from zinc acetate dihydrate, but annealing temperatures of 750 °C were necessary to achieve this level of performance. Only the work of Ahmad *et al*.,[30] on solution-processed small-molecule organic Schottky diodes based on methyl-red, reported current rectification ratios approaching 10^6 at ±1.1 V.

We note that the current rectification ratio values achieved here exceeds even those of ZnO Schottky diodes fabricated via vacuum-based techniques such as molecular beam epitaxy (MBE) and sputtering for which typically values fall in the range of 10^3-10^4 [31–35] , with the highest current rectification ratio of ~10^5 reported for high temperature annealed sputtered ZnO Schottky diodes.[36] Only devices fabricated on bulk single crystal ZnO, or on high quality ZnO layers grown using pulsed laser deposition (PLD), demonstrate superior current rectification. For example, Nakano *et al*.[37] fabricated poly(3,4-ethylenedioxythiophene): poly(styrenesulfonate) (PEDOT:PSS) Schottky contacts on 0001 single crystal ZnO with rectification ratios of 10^9 at ±2 V. Similarly, Allen *et al*.[38] achieved current rectification values of up to 10^9 by depositing silver oxide Schottky contacts on the Zn polar surface of ZnO wafers, while Müller *et al*.[39] reported a maximum rectification ratio value of 7×10^{10} for Schottky diodes based on PLD-grown ZnO and sputtered PdOx contact.

There are two main reasons for the high rectification ratios achieved in our coplanar ZnO Schottky diodes [**Figure 1(c)**]. Firstly, the quality of the ZnO layers processed from the carbon-free $Zn(OH)_x(NH_3)_y^{(2-x)+}$ precursor solutions appear to be excellent exhibiting high electron mobility (10 cm^2/Vs) due to their continuous polycrystalline nature[5,18,40] . Secondly, the coplanar

asymmetric Au/Al electrodes architecture employed is rather unique and can be realized at such scale only via a-Lith.[16,17] By adopting the coplanar electrode geometry, we ensure that no electrical shorts form between the Schottky (Au) and Ohmic (Al) contacts, which as already discussed often occur during deposition of the top metal contact in conventional sandwich (staggered) diodes, while maintaining the extremely small inter-electrode (nano-gap) distance of <20 nm [**Figure 1(A)**].[17] The latter feature helps to minimize the device's series resistance and hence maintain the RC constant at ultra-low levels. The combination of these unique characteristics make the proposed coplanar architecture highly interesting for numerous applications in high-frequency electronics fabricated even on inexpensive substrate materials such as plastic.[16]

3.2. Charge Carrier Injection and Transport

Figure 1 (D) shows a log-log plot of the forward biased I-V characteristic (0-2.5 V) shown in **Figure 1(C)**. As can be seen, there are three distinct electron transport regions. Each region is assigned to a different charge injection/transport mechanism. For example, in region I, the slope of the plot is <1 most likely indicating tunneling as the dominant charge transport mechanism.[41] As the bias increases (region II), the current-voltage relationship becomes exponential, indicating the prevalence of thermionic emission, as would be expected in a Schottky diode.[27] At even higher voltages (region III) the slope becomes ~4.4. The characteristic $I \propto V^n$ ($n > 2$) relationship indicates trap assisted space charge limited current (SCLC) as the predominant charge transport mechanism.[42] On the basis of these observations we expect the diode current (I) in region II to follow the well-known thermionic emission theory given as:[15]

$$I = I_0 e^{\frac{qV}{nkT}} \quad (2)$$

where n is the diode ideality factor and I_0 is the reverse bias saturation current given by $I_0 = SA^*T^2e^{-\frac{q\Phi_B}{kT}}$. Here, A^* is the effective Richardson constant and S is the diode cross-sectional area. Applying this basic model to our devices yields barrier heights for electrons of 0.79 eV and a diode ideality factor of 1.9. We note that these extracted values compare favorably with state-of-the-art solution-processed ZnO Schottky diodes reported recently.[20,23]

Another important parameter that needs to be considered in this analysis is the device series resistance. The latter can be extracted following the method of Cheung *et al*.[43] In their approach, **Eq. 2** can be expanded to include the effect of series resistance and is given as:

$$\frac{dV}{d(\ln I)} = \frac{nkT}{q} + IR_S \quad (3)$$

To evaluate Φ_B, a function H(I) is defined:

$$H(I) \equiv V - \left(\frac{nkT}{q}\right)\ln\left(\frac{I}{SAT^2}\right) \quad (4)$$

and it follows that

$$H = n\Phi_B - IR_S \quad (5)$$

Eq. 5 can be used to evaluate Φ_B and a second approximation of the diode's series resistance. **Figures 2(A-B)** show the Cheung plots for the thermionic emission region which yield a barrier height value of Φ_B = 0.54 eV, and first and second approximations of the series resistance of 28 kΩ and 32 kΩ, respectively. To this end, reported values of the series resistance for ZnO Schottky diodes vary significantly from Ohms[32] to kilo Ohms.[27] The diodes' ultra-small active area of

~5×10^{-11} m^{-2} [taken as the product of the electrode thickness (~40 nm) times the circumference (1 mm) of the circular Au electrode in **Figure 1(B)**] here is believed to be the cause for the high series resistance value obtained. However, since the forward current scales with the diode's nano-gap width[16]it is expected that devices with larger width will exhibit reduced series resistance. Moderate *n*-doping of ZnO[44,45] may also be explored as an alternative approach for improving the diode's performance.

3.3. Temperature Dependent Electron Transport Analysis

Measurement of the temperature dependence of the I-V (I-V-T) characteristics is another method that can be used to evaluate Φ_B, but also estimate the effective Richardson constant (A^*). **Figure 3(A)** displays the I-V characteristics of a coplanar ZnO Schottky diode measured at temperatures in the range 80-320 K. Using these data the standard Richardson plot can be obtained by plotting $\ln\left(\frac{I_0}{ST^2}\right)$ versus $\frac{1}{kT}$. The corrected form of the plot may also be obtained by plotting $\ln\left(\frac{I_0}{ST^2}\right)$ against $\frac{1}{nkT}$. We do note, however, that these models do not take into account the temperature dependence of n and Φ_B. Bhuiyan *et al*.[46] derived a model taking into account this dependence, where the ideality factor, $n(T)$, and $\Phi_B(T)$ are given empirically by:

$$\mathrm{n(T)} = \mathrm{a} + \frac{\mathrm{b}}{\mathrm{T}} \tag{6}$$

$$\Phi_B(T) = \Phi_{B0} - \alpha T \tag{7}$$

Here Φ_{B0} is the apparent barrier height at $T = 0$, a and b are constants and T is the temperature. **Eq. 7** allows calculation of the apparent Φ_{B0} but not of the true flat-band barrier height (Φ_{Bfb}). The latter may be obtained using:

$$\Phi_{Bfb} = n\Phi_B - (n-1)\frac{kT}{q} ln \frac{N_C}{N_D} \quad (8)$$

where N_C is the density of states in the conduction band and N_D is the carrier concentration. The modified saturation current then becomes:

$$n(T) ln\left(\frac{I_0}{ST^2}\right) = -\frac{1}{kT}(\Phi_B - kb\ln(A)) + a\ln(A) + \frac{\alpha}{k} \quad (9)$$

Figure 3 (B) shows a plot of $n(T)\ln\left(\frac{I_0}{ST^2}\right)$ vs. $\frac{1}{kT}$. Values for S, α and b are extracted from the plots of $n(T)$ and $\Phi_B(T)$ versus T shown in the inset in the same figure. The best fit for the data [solid line in **Figure 3(B)**] yields a value for A^* = 38.9 A cm^{-2} K^{-2} and the barrier heights at $T = 0$ K (Φ_{B0}) and T = 300 K (Φ_B) of 0.88 eV and 0.84 eV, respectively. The Φ_B value is in good agreement with the value extracted from the I-V analysis and falls within the range of previously reported barrier heights extracted via I-V-T analysis for different Schottky contacts (see **Table I**).

Table I. Comparison of Φ_B and Richardson constant values extracted via I-V-T measurements for ZnO Schottky diodes grown using different methods.

ZnO growth method	**Schottky contact material**	Φ_B **(eV)**	**Temperature Range (K)**	**Richardson Constant (A cm^{-2} K^{-2})**	**Ref.**
Melt grown wafer	IrOx	0.91	293 – 440	27	[47]

Nanowires (wet chemical route)	Pd	1.25	303 – 383	17.2	[48]
Bulk single crystal	Pd	0.61	80 – 180	167	[49]
Thermal evaporation	Pd	1.41	300 – 423	19.54	[50]
Solution $Zn(O_2CCH_3)_2{\cdot}(H_2O)_2$	Pd	1.39	294 – 493	31.67	[51]
Hydrothermal	AgOx	1.19	293 – 423	10	[38]
Bulk single crystal	Ag	0.82	240 – 440	0.248	[52]
Bulk single crystal	Pd	0.97	140 –200	39.43	[53]
			210 – 300	39.03	
Hydrothermal	Ag	0.97	200 – 300	88.1	[54]
		0.48	100 – 180	51.5	
This work	Au	0.89	80 – 320	38.9	

Interestingly, the extracted value of A^* is remarkably similar to its theoretical value of 32 A cm^{-2} K^{-2} calculated assuming an effective electron mass in ZnO of 0.275 m_e.[23,55,56] It is also in excellent agreement with values reported for best-performing ZnO Schottky diodes reported to date (**Table I**). To this end, it is worth noting that most researchers consider a Gaussian distribution of barrier heights when analyzing I-V-T data for ZnO Schottky barriers. The latter approach yields different values of Φ_B and A^* for different temperature ranges, with some studies proposing the existence of a double Gaussian distribution as a possible explanation.[53,54] However, the model we have adopted here yields consistent values through the temperature range of 80-320 K investigated and thus may offer a more valid depiction of the temperature dependence of the Schottky barrier.

3.4. Capacitance-Voltage Characterisation

Capacitance-voltage (C-V) measurements provide an alternative method in determining the Schottky barrier height.[15] This approach is considered to be the most practical since allows the value of Φ_{Bfb} to be calculated while the effect of image force lowering remains negligible. Moreover, the effective doping density, (N_D) may also be determined, providing further insights into the fundamental processes at play. Under ideal behavior, the diode capacitance (C_{diode}) as a function of applied voltage (V) is given by:

$$C_{diode} = S\left(\frac{q\varepsilon_0\varepsilon_S N_D}{2\left(V_{bi}-V-\frac{kT}{q}\right)}\right)^{1/2} \tag{10}$$

where V_{bi} is the built-in potential, S is the diode's cross-sectional area and ε_S is the dielectric constant of the semiconductor. In coplanar diodes it is useful to first consider the effect of the empty nano-gap capacitance (C_{empty}). The reasoning for this becomes clear when considering the intrinsic capacitance of the apparent active area of the diode taken as the product of the electrode thickness (40 nm) times the circumference (1 mm) of the circular Au electrode in **Figure 1(B)**. Based on this geometry and assuming an inter-electrode nano-gap of 20 nm, one would expect a value of the capacitance on the order of 10^{-14} F. However we have previously reported this experimentally determined value to be on the order of 0.2 pF.[16] The reason for this is the existence of an extrinsic capacitance contribution due to 3D coupling of the electrodes, which has not been taken into consideration. De Vries *et al*. [57] devised an approximation for the extrinsic capacitance per unit length of coplanar electrodes using conformal mapping as:

$$C_{empty}/_{l} = \frac{\varepsilon_r\varepsilon_0}{\pi} ln\left(\frac{8W}{d}\right) \tag{11}$$

In **Eq. 11** W represents the width of the electrodes themselves [i.e. not the width of the channel, but the diameter of the circular Au electrode in **Figure 1(A)**] and d is again the electrode separation (nano-gap length). This prediction gives a value of capacitance of ≈ 0.2 pF for the empty gap extrinsic capacitance assuming a value of ε_r~4.6 for glass. We note however that the latter value may vary significantly depending the specific composition of the glass substrates used. In measuring the C-V characteristics of the coplanar ZnO Schottky nanojunction diodes, the C^{-2} values have thus been corrected for this value by subtracting the measured value of C_{empty} from C_{diode}.

Figure 4(A) shows a plot of corrected $1/C^2$ versus applied bias (V) measured using a small AC signal with frequency of 10 kHz and 1 MHz. From this plot, both the N_D and V_{bi} can be extracted. **Figure 4(B)** shows the evolution of N_D as a function of frequency from 5 kHz to 1 MHz at room temperature. Interestingly, the value of N_D increases from ~0.71×10^{18} cm^{-3} at 5 kHz to 1.38×10^{18} cm^{-3} at 1 MHz. Similar behaviour has previously been observed in conventional ZnO Schottky diodes and has been attributed to the inability of interface states at the Schottky barrier to trap charge carriers at higher frequencies.[58,59] While thus not unique to the planar architecture, the implications for employing these devices in high frequency applications such as DC rectifiers is extremely positive, as the device performance appears to improve at higher frequencies.V_{bi} is also seen to increase with increasing frequency, and is also attributed to the screening of traps present at the critical interface.[58] Using the C-V data, Φ_B can then be determined employing the relationship:

$$\Phi_B = V_{bi} + \frac{kT}{q}\ln\left(\frac{N_C}{N_D}\right) \tag{12}$$

To improve the degree of accuracy, V_{bi} and Φ_B were calculated at 1 MHz where the effect of electron trapping is minimum [**Figure 4(B)**] yielding values of 0.86 eV and 0.89 eV, respectively. Both values agree well with those extracted via I-V and I-V-T analysis. **Table II** summarizes the values for Φ_B obtained from the different methods together with various other junction parameters.

Table II. Junction properties calculated for the coplanar Au/ZnO Schottky diodes.

Schottky Contact	**Φ_B (eV)**				**n**	**R_S (kΩ)**	**A* (A cm^{-2} K^{-2})**	**N_D (cm^{-3})**
	I-V	**C-V**	**I-V-T**	**Cheung[43]**				
Au	0.79	0.89	0.84	0.54	1.9	28 32	38.9	1.4×10^{18}

4. Conclusion

We reported the fabrication and electrical characterisation of solution-processed coplanar ZnO-based Schottky diodes with unprecedented current rectification ratios (>10^6) and low voltage operation (<2.5 V). The superior diode performance is attributed to the unique coplanar nano-gap architecture employed featuring two asymmetric (Au/ZnO/Al) metal electrodes patterned via adhesion-lithography[17] and the formation of a rectifying Schottky contact for electrons at the Au/ZnO interface. To gain a better understanding of the current rectification mechanism, the barrier height for electrons was analyzed using a combination of I-V, I-V-T and C-V techniques and found to be in the range 0.54-0.89 eV. A model taking into account the temperature dependence of the barrier height and ideality factor of the diode was employed to extract the Richardson constant over the temperature range of 80-320 K yielding a value of A^* = 38.9 A cm^{-2} K^{-2}. This value is in excellent agreement with both the theoretically predicted value of 32 A cm^{-2}

K^{-2}, and experimental values reported previously for state-of-the-art ZnO Schottky diodes. Finally, using capacitance-voltage measurements, we show that electron traps present at the Au/ZnO interface, and/or within ZnO, become less significant at higher frequencies, where the apparent free electron concentration appears to increase. The latter characteristic makes the coplanar Au/ZnO/Al Schottky nanojunction diodes developed here attractive for application in high frequency, large-area electronics that can be manufactured from solution phase on arbitrary substrate materials such as plastic.

FIGURES

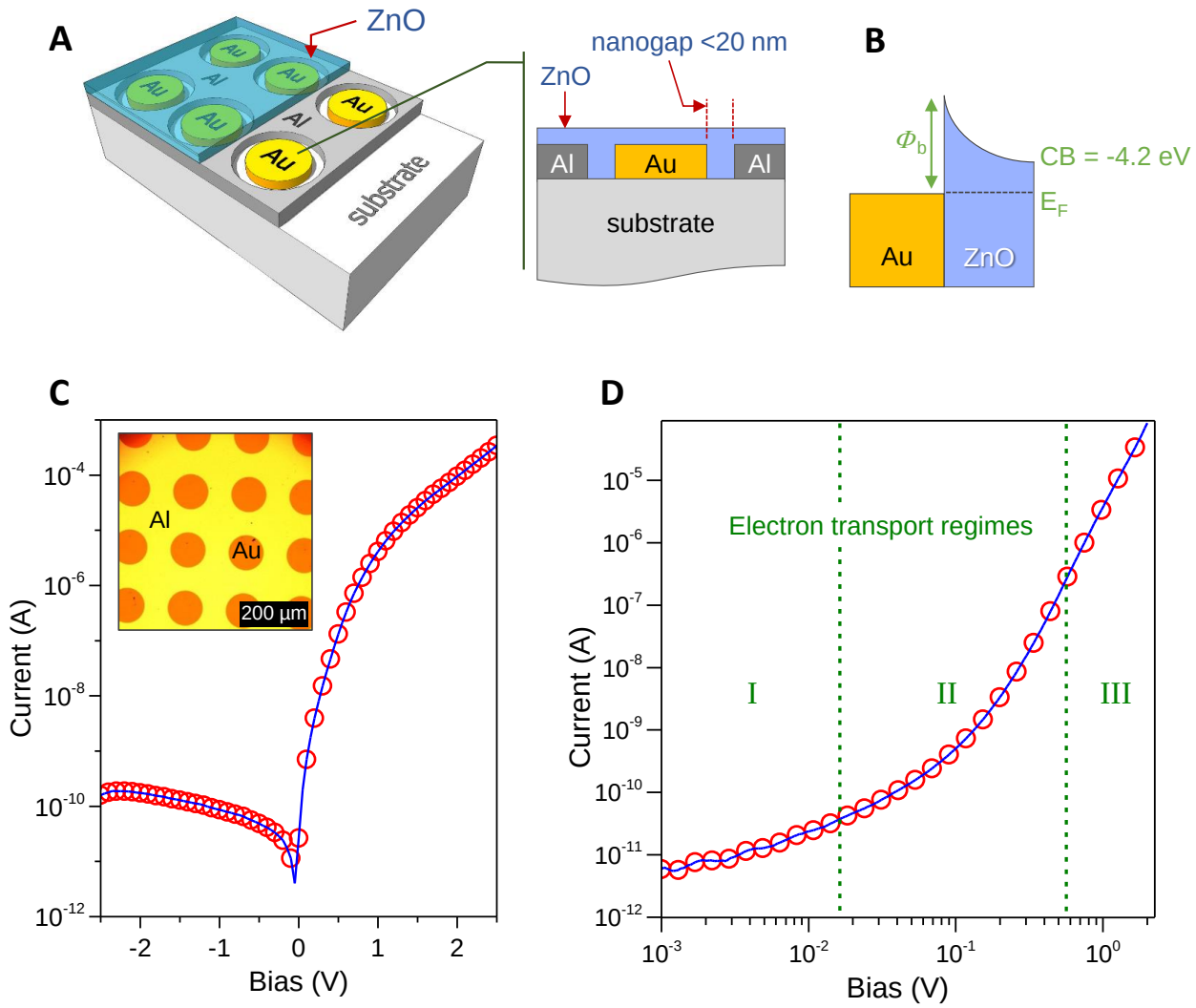

Figure 1. (a) 3D schematic of the device architecture and its cross-section. (b) Energy band diagram of the Schottky contact formed between the Au contact and ZnO. (c) Current-voltage characteristics shown in semi-log plot. Inset: Microscope image of the actual Schottky diodes array studied. (d) Forward current-voltage characteristics shown in log-log plot and corresponds to measurements performed when the positive potential bias is applied to the Schottky (Au) contact.

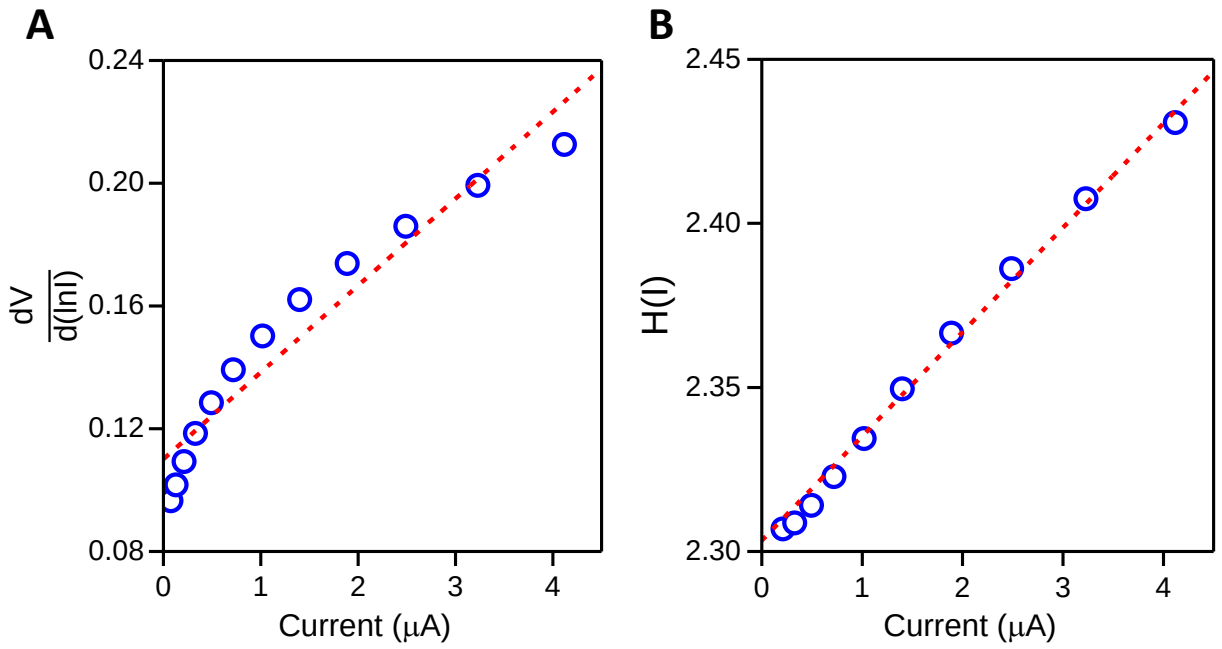

Figure 2. Cheung plots. (a) $dV/d(\ln I)$ versus diode current for the extraction of R_S. (b) H(I) versus current for a second approximation of R_S and the extraction of barrier height.

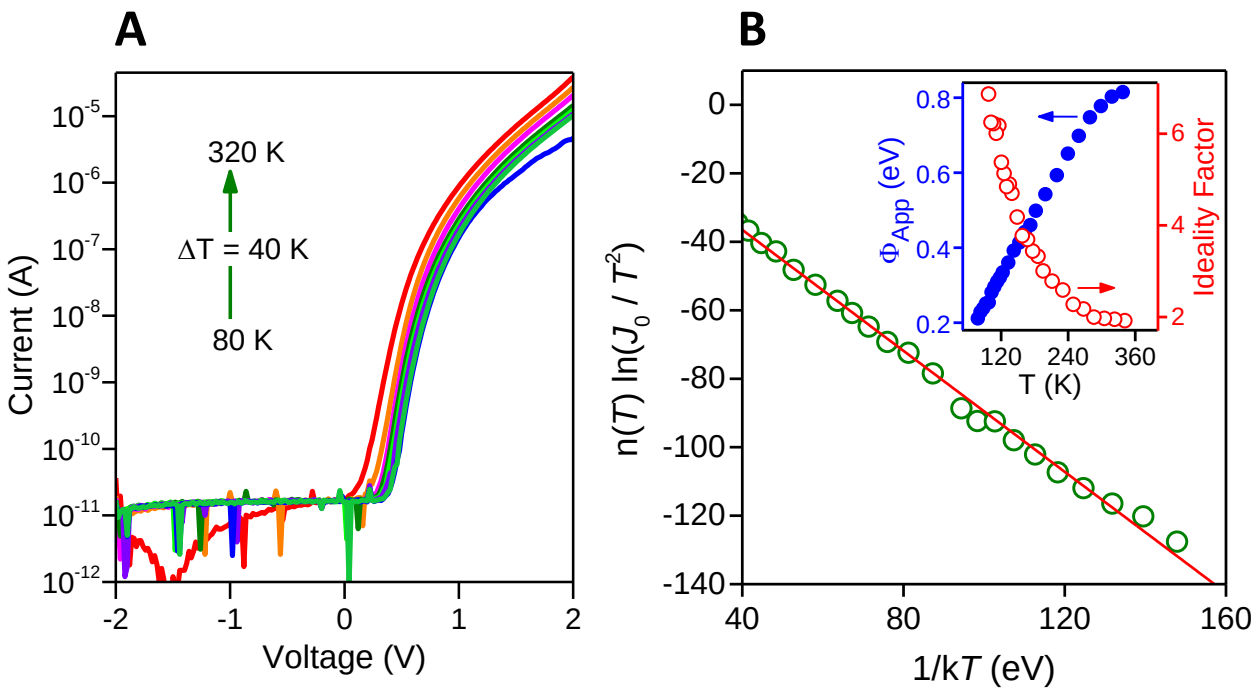

Figure 3. (a) Temperature dependence (80-320 K) of the current-voltage characteristics measured for a representative coplanar ZnO Schottky coplanar nanojunction. (b) Richardson plot using the model of Bhuiyan *et al*. Inset shows the temperature dependence of the ideality factor and barrier height (Φ_{App}). Forward bias corresponds to a positive bias being applied to the Schottky (Au) contact.

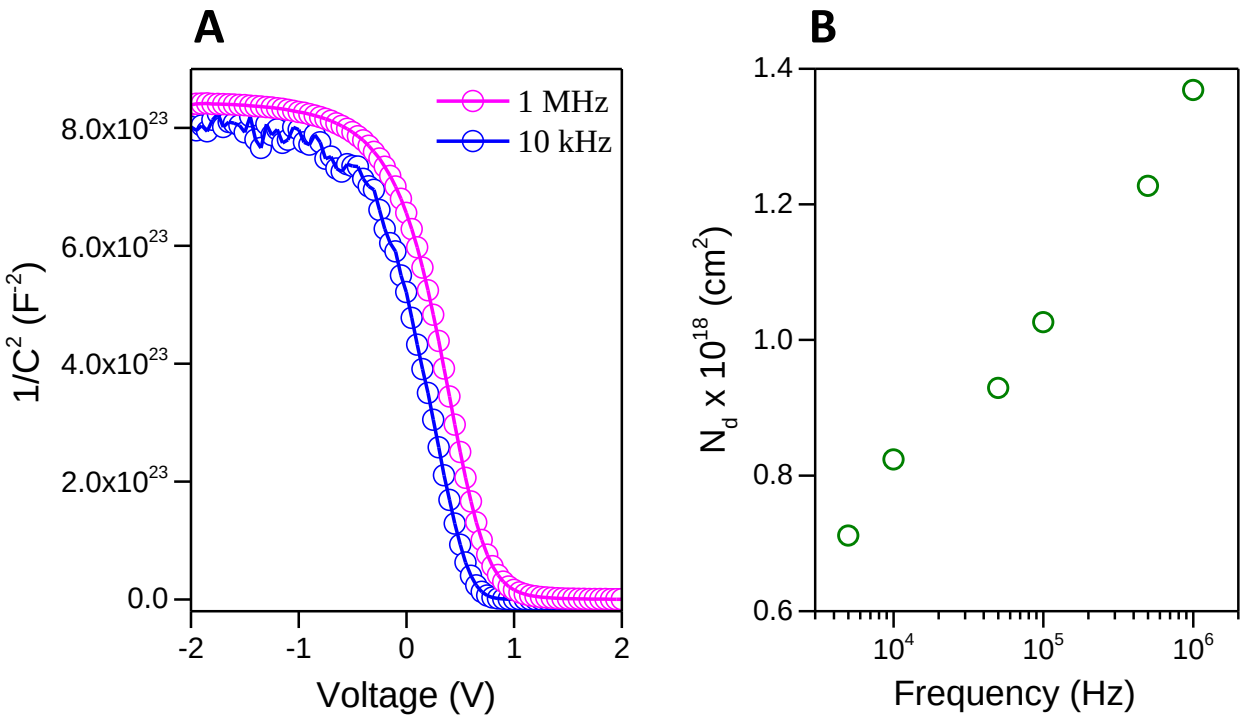

Figure 4. (a) Representative C^{-2} vs. V plots measured at 10 kHz and 1 MHz. (b) Variation of extracted values of N_D as a function of frequency.

.

AUTHOR INFORMATION

Corresponding Author

*Email: thomas.anthopoulos@imperial.ac.uk

Author Contributions

The manuscript was written through contributions of all authors. All authors have given approval to the final version of the manuscript.

Funding Sources

The authors are grateful to the European Research Council (ERC) AMPRO grant number 280221 and the Engineering and Physical Sciences Research Council (EPSRC) grant number EP/P505550/1 and the EPSRC Centre for Innovative Manufacturing in Large Area Electronics (CIM-LAE) grant no. EP/K03099X/1 for financial support.

REFERENCES

1. Yadav, A.; Pandey, A.; Somvanshi, D.; Jit, S. Sol-Gel-Based Highly Sensitive Pd/n-ZnO Thin Film/n-Si Schottky Ultraviolet Photodiodes. *IEEE Trans. Electron Devices* **2015**, *62*, 1879-1884.

2. Lee, B.; Kim, C.; Lee, Y.; Lee, S.; Kim, D. Y. Dependence of Photocurrent on UV Wavelength in ZnO/Pt Bottom-Contact Schottky Diode. *Curr. Appl. Phy.* **2015**, *15,* 29-33.

3. Nasiri, N.; Bo, R.; Wang, F.; Fu, L.; Tricoli, A. Ultraporous Electron-Depleted ZnO Nanoparticle Networks for Highly Sensitive Portable Visible-Blind UV Photodetectors. *Adv. Mater.* **2015**, *27*, 4336–4343.

4. Vanmaekelbergh, D.; van Vugt, L. ZnO Nanowire Lasers. *Nanoscale* **2011**, *3*, 2783-27800.

5. Lin, Y.; Faber, H.; Zhao, K.; Wang, Q.; Amassian, A.; McLachlan, M.; Anthopoulos, T. D. High-Performance ZnO Transistors Processed Via an Aqueous Carbon-Free Metal Oxide Precursor Route at Temperatures Between 80–180 °C. *Adv. Mater.* **2013**, *25*, 4340–4346.

6. Wang, Z.; Song, J. Piezoelectric Nanogenerators Based on Zinc Oxide Nanowire Arrays. *Science* **2006**, *312*, 242–246.

7. Singh, R.; Cooper, J. A.; Melloch, M. R.; Chow, T. P.; Palmour, J. W. SiC Power Schottky and PiN Diodes. *IEEE Trans. Electron Devices* **2002**, *49*, 665–672.

8. Yakuphanoglu, F.; Basaran, E.; Şenkal, B. F.; Sezer, E. Electrical and Optical Properties of an Organic Semiconductor Based on Polyaniline Prepared by Emulsion Polymerization and Fabrication of Ag/Polyaniline/n-Si Schottky Diode. *J. Phys. Chem. B* **2006**, *110*, 16908–16913.

9. Maestrini, A.; Thomas, B.; Wang, H.; Jung, C.; Treuttel, J.; Jin, Y.; Chattopadhyay, G.; Mehdi, I.; Beaudin, G. Schottky Diode-Based Terahertz Frequency Multipliers and Mixers. *C. R. Phys.* **2010**, *11*, 480–495.

10. Crowell, C. R.; Sze, S. M. Current Transport in Metal-Semiconductor Barriers. *Solid-State Electron.* **1966**, *9*, 1035–1048.

11. Rideout, V. L.; Crowell, C. R. Effects of Image Force and Tunneling on Current Transport in Metal-Semiconductor (Schottky Barrier) Contacts. *Solid-State Electron.* **1970**, *13*, 993–1009.

12. Brillson, L.; Lu, Y. ZnO Schottky Barriers and Ohmic Contacts. *Journal of Applied Physics* **2011**, *109*, 121-301.

13. Monakhov, E. V.; Kuznetsov, Y.; Svensson B. G. Zinc Oxide: Bulk Growth, Role of Hydrogen and Schottky Diodes. *Journal of Physics D: Applied Physics* **2009**, *42*, 153001.

14. Özgür, Ü.; Alivov, Y.; Liu; Teke; Reshchikov, Ma.; an, D.; Avrutin, V.; Cho, S.-J.; Morkoc A Comprehensive Review of ZnO Materials and Devices. *J. Appl. Phys.* **2005**, *98*, 041301.

15. Sze, S. M.; Ng, K. Physics of Semiconductor Devices. *John Wiley & Sons* **2006**, Third Edition, Hoboken, NJ, USA, pp 136–139.

16. Semple, J.; Rossbauer, S.; Burgess, C.; Zhao, K.; Jagadamma, L.; Amassian, A.; McLachlan, M.; Anthopoulos, T. D. Radio Frequency Coplanar ZnO Schottky Nanodiodes Processed from Solution on Plastic Substrates. *Small* **2016,** *12*, 1993-2000.

17. Beesley, D. J.; Semple, J.; Jagadamma, L.; Amassian, A.; McLachlan, M. A.; Anthopoulos, T. D. Sub-15-Nm Patterning of Asymmetric Metal Electrodes and Devices by Adhesion Lithography. *Nat. Commun.* **2014**, *5,* 3933.

18. Lin, Y.; Faber, H.; Labram, J.; Stratakis, E.; Sygellou, L.; Kymakis, E.; Hastas, N.; Li, R.; Zhao, K.; Amassian, A.; Treat, N. D.; McLachlan, M.; Anthopoulos, T. D. High Electron Mobility Thin-Film Transistors Based on Solution-Processed Semiconducting Metal Oxide Heterojunctions and Quasi-Superlattices. *Adv Sci* **2015**, *2*, 1500058.

19. Yilmaz, M.; Caldiran, Z.; Deniz, A. R.; Aydogan, S.; Gunturkun, R.; Turut A. Preparation and Characterization of Sol–gel-Derived n-ZnO Thin Film for Schottky Diode Application. *Appl. Phys. A* **2015**, *119*, 547-552.

20. Hwang J.; Kung C.; Lin Y. Non-Surface-Treated Au/ZnO Schottky Diodes Using Pre-Annealed Hydrothermal or Sol-Gel Seed Layer. *IEEE Trans. Nanotechnol.* **2013,** *12,* 35-39.

21. Yadav A. B.; Periasamy C.; Bhaumik S. Hydrogen Gas Sensing Properties of Pd/ZnO Thin Films Grown on N-Si< 100> Substrates at Room-Temperature by Thermal Evaporation and Sol-Gel Techniques: A Comparative Study. *Indian J. Pure Appl. Phys.* **2013**, *51*, 792-799.

22. Singh, B.; Tripathi, S. Fabrication and Characterization of Au/p-ZnO Schottky Contacts. *Superlattices Microstruct.* **2015**, *85*, 697–706.

23. Middya, S.; Layek, A.; Dey, A.; Datta, J.; Das, M.; Banerjee, C.; Ray, P. Role of Zinc Oxide Nanomorphology on Schottky Diode Properties. *Chem. Phys. Lett.* **2014,** *610,* 39-44.

24. Han K. J.; Kang K. S.; Chen Y.; Yoo, K. H.; Kim, J. Effect of Annealing Temperature on the Conduction Mechanism for a Sol–gel Driven ZnO Schottky Diode. *J. Phys. D: Appl. Phys.* **2009**, *42*, 125110.

25. Kim, K.; Song, Y. W.; Leem, J.; Kim, S. Preparation and Analysis of Schottky Diodes with Au and Sol-Gel-Processed ZnO Thin Films. *J. Kaorean Phys. Soc.* **2009,** *55*, 140-143.

26. Mansour, S.; Yakuphanoglu, F. Electrical-Optical Properties of Nanofiber ZnO Film Grown by Sol Gel Method and Fabrication of ZnO/p-Si Heterojunction. *Solid State Sci.* **2012**, *14*, 121–126.

27. Farag, A. A. M.; Farooq, W. A.; Yakuphanoglu F. Characterization and Performance of Schottky Diode Based on Wide Band Gap Semiconductor ZnO Using a Low-Cost and Simplified Sol–gel Spin Coating Technique. *Microelectron. Eng.* **2011**, *88*, 2894–2899.

28. Yakuphanoglu, F. Electrical Characterization and Device Characterization of ZnO Microring Shaped Films by Sol–gel Method. *J. Alloys Compd.* **2010**, *507*, 184–189.

29. Chen, Y.; Jyoti, N.; Hyun-U, K.; Kim, J. Effect of Annealing Temperature on the Characteristics of ZnO Thin Films. *J. Phys. Chem. Solids* **2012**, *73*, 1259–1263.

30. Ahmad, Z.; Sayyad, M. H. Electrical Characteristics of a High Rectification Ratio Organic Schottky Diode Based on Methyl Red. *Optoelectron. Adv. Mater., Rapid Commun.* **2009**, *3*, 509–512.

31. Wenckstern, H. von; Müller, S.; Biehne, G.; Hochmuth, H.; Lorenz, M.; Grundmann, M. Dielectric Passivation of ZnO-Based Schottky Diodes. *J. Electron. Mater.* **2010**, *39*, 559–562.

32. Zhang, X.; Zhai, J.; Yu, X.; Ding, L.; Zhang, W. Fabrication and Characterization of Flexible Ag/ZnO Schottky Diodes on Polyimide Substrates. *Thin Solid Films* **2013**, *548*, 623–626.

33. Dhananjay; Nagaraju, J.; Krupanidhi, S. B. Investigations on Magnetron Sputtered ZnO Thin Films and Au/ZnO Schottky Diodes. *Phys. B.* **2007**, *391*, 344–349.

34. Lin, T. K.; Chang, S. J.; Su, Y. K.; Huang, B. R.; Fujita, M.; Horikoshi, Y. ZnO MSM Photodetectors with Ru Contact Electrodes. *J. Cryst. Growth* **2005**, *281*, 513–517.

35. Asghar, M.; Mahmood, K.; Rabia, S.; Samaa, B. M.; Shahid, M. Y.; Hasan, M. A. Investigation of Temperature Dependent Barrier Height of Au/ZnO/Si Schottky Diodes. *IOP Conf. Ser.: Mater. Sci. Eng.* **2014**, *60*, 012041.

36. Alivov, Y.; Bo, S.; Akarca-Biyikli, X.; Fan, Q.; Xie, J.; Biyikli, N.; Zhu, K.; Johnstone, D.; Morkoç, H. Effect of Annealing on Electrical Properties of Radio-Frequency-Sputtered ZnO Films. *J. Electron. Mater.* **2006**, *35*, 520–524.

37. Nakano, M.; Makino, T.; Tsukazaki, A.; Ueno, K.; Ohtomo, A.; Fukumura, T.; Yuji, H.; Akasaka, S.; Tamura, K.; Nakahara, K.; Tanabe, A.; Kamisawa A.; Kawasaki, M. Transparent Polymer Schottky Contact for a High Performance Visible-Blind Ultraviolet Photodiode Based on ZnO. *Appl. Phys. Lett.* **2008**, *93*, 123309.

38. Allen, M. W.; Weng, X.; Redwing, J. M.; Sarpatwari, K.; Mohney, S. E.; von Wenckstern, H.; Grundmann, M.; Durbin S. M. Temperature-Dependent Properties of Nearly Ideal ZnO Schottky Diodes. *IEEE Trans. Electron Devices* **2009,** *56*, 2160-2164.

39. Müller, S.; Wenckstern, H. von; Schmidt, F.; Splith, D.; Heinhold, R.; Allen, M.; Grundmann, M. Method of Choice for Fabrication of High-Quality ZnO-Based Schottky Diodes. *Journal of Applied Physics* **2014**, *116*, 194506.

40. Meyers, S. T.; Anderson, J. T.; Hung, C. M.; Thompson, J.; Wager, J. F.; Keszler, D. A. Aqueous Inorganic Inks for Low-Temperature Fabrication of ZnO TFTs. *J. Am. Chem. Soc.* **2030**, *130*, 17603–17609.

41. Mahmood, F. S.; Gould, R. D.; Hassan, A. K.; Salih, H. M. D.C. Properties of ZnO Thin Films Prepared by R.f. Magnetron Sputtering. *Thin Solid Films* **1995**, *270*, 376–379.

42. Rose, A. Space-Charge-Limited Currents in Solids. *Phys. Rev.* **1955**, *97*, 1538.

43. Cheung, S.; Cheung, N. Extraction of Schottky Diode Parameters from Forward Current-Voltage Characteristics. *Appl. Phys. Lett.* **1986**, *49,* 85-87.

44. Lin, Y.; Thomas, S.; Faber, H.; Li, R.; McLachlan, M.; Patsalas, P.; Anthopoulos, T. D. Al-Doped ZnO Transistors Processed from Solution at 120 °C. *Adv. Electron. Mater.* **2016**, *2*, 1600070.

45. Rossbauer, S.; Müller, C.; Anthopoulos, T. D. Comparative Study of the N-Type Doping Efficiency in Solution-processed Fullerenes and Fullerene Derivatives. *Adv. Funct. Mater.* **2014**, *24*, 7116–7124.

44. Bhuiyan, A. S.; Martinez, A.; Esteve D. A New Richardson Plot for Non-Ideal Schottky Diodes. *Thin Solid Films* **1988**, *161*, 93–100.

46. Sarpatwari, K.; Awadelkarim, O. O.; Allen, M. W.; Durbin, S. M.; Mohney S. E. Extracting the Richardson Constant: IrOx/n-ZnO Schottky Diodes. *Appl. Phys. Lett.* **2009**, *94*, 242110.

47. Gayen, R. N.; Bhattacharyya, S. R.; Jana P. Temperature Dependent Current Transport of Pd/ZnO Nanowire Schottky Diodes. *Semicond. Sci. Technol.* **2014**, *29*, 095022.

48. Mtangi, W.; Auret, F. D.; Nyamhere, C. Analysis of Temperature Dependent I–V Measurements on Pd/ZnO Schottky Barrier Diodes and the Determination of the Richardson Constant. *Phys. B* **2009,** *404,* 1092-1096.

49. Somvanshi, D.; Jit, S. Mean Barrier Height and Richardson Constant for Pd/ZnO Thin Film-Based Schottky Diodes Grown on N-Si Substrates by Thermal Evaporation Method. *IEEE Electron Device Lett.* **2013**, *34,* 1238-1240.

50. Yadav, A.; Pandey, A; Jit, S. Pd Schottky Contacts on Sol–Gel Derived ZnO Thin Films with Nearly Ideal Richardson Constant. *IEEE Electron Device Lett.* **2014**, *35*, 729–731.

51. Gür, E.; Tüzemen; Kiliç, B.; Coşkun C. High-Temperature Schottky Diode Characteristics of Bulk ZnO. *J. Phys.: Condens. Matter* **2007**, *19*, 196206.

52. Mayimele, M.; Diale, M.; Mtangi, W.; Auret, F. Temperature-Dependent Current–voltage Characteristics of Pd/ZnO Schottky Barrier Diodes and the Determination of the Richardson Constant. *Mater. Sci. Semicond. Process.* **2015**, *34*, 359-364.

53. Kim, H.; Sohn, A.; Cho, Y.; Kim, D.-W. Temperature-Dependent Electrical Characteristics of Ag Schottky Contacts to Differently Grown O-Polar Bulk ZnO. *J. Electron. Packag.* **2013**, *135*, 011010.

54. Lai, B.; Lee, C.; Hong, J.; Yao S. Zinc Oxide-Based Schottky Diode Prepared Using Radio-Frequency Magnetron Cosputtering System. *Jpn. J. Appl. Phys.* **2010,** *49***,** 085501.

55. Faraz, S.; Willander, M.; Wahab Q. Current Transport Studies and Extraction of Series Resistance of Pd/ZnO Schottky Diode. *Multitopic Conference (INMIC), 2011 IEEE 14th International*, Karachi, **2011**, 196–200.

56. de Vries, D.; Stelmaszyk, P.; Wieck A. D. Intrinsic and Extrinsic Capacitances of in Plane Gated Transistors. *J. Appl. Phys.* **1996**, *79*, 8087–8090.

57. Alim, M.; Seitz, M.; Hirthe, R. Complex Plane Analysis of Trapping Phenomena in Zinc Oxide Based Varistor Grain Boundaries. *J. Appl. Phys.* **1988**, *63*, 2337–2345.

58. Benhaliliba, M.; Ocak, Y.S.; Mokhtari, H.; Kiliçoglu, T. AC impedance analysis of the Al/ZnO/p-Si/Al Schottky diode: C-V plots and extraction of parameters *J. Nano- Electron. Phy.* **2015,** *7*, 1-4.

59. Farag, A. A. M.; Farooq, W. A.; Yakuphanoglu, F. Characterization and performance of Schottky diode based on wide band gap semiconductor ZnO using a low-cost and simplified sol-gel spin coating technique *Microelectron. Eng.* **2011**, *88*, 2894-2899.

Table of Contents Figure